Acta Chemica Scandinavica, 1996: 50: 906–913
Printed in UK – all rights reserved

ACTA
CHEMICA SCANDINAVICA
ISSN 0904-213X

Enantiomer Associations in the Crystal Structures of Racemic and (2*S*,3*R*)-(−)-3-Hydroxy-2-(4-methoxyphenyl)-2,3-dihydro-1,5-benzothiazepin-4(5*H*)-one

Katalin Marthi,[a] Sine Larsen,[a] Mária Ács,[†,b] Zsuzsa Jászay[b] and Elemér Fogassy[b]

[a]Centre for Crystallographic Studies,[‡] Department of Chemistry, University of Copenhagen, Universitetsparken 5, DK-2100 Copenhagen, Denmark and [b]Department of Organic Chemical Technology, Technical University of Budapest, P.O. Box 91, H-1521 Budapest, Hungary

Marthi, K., Larsen, S., Ács, M., Jászay, Zs. and Fogassy, E., 1996. Enantiomer Associations in the Crystal Structures of Racemic and (2*S*,3*R*)-(−)-3-Hydroxy-2-(4-methoxyphenyl)-2,3-dihydro-1,5-benzothiazepin-4(5*H*)-one. – Acta Chem. Scand. 50: 906–913. © Acta Chemica Scandinavica 1996.

The crystal structures of racemic and (2*S*,3*R*)-(−)-3-hydroxy-2-(4-methoxyphenyl)-2,3-dihydro-1,5-benzothiazepin-4(5*H*)-one ($C_{16}H_{15}NO_3S$) have been determined in order to compare the interactions between molecules of the same and opposite chirality. The enantiomeric associations observed in these two crystal structures are analysed, relating the differences to those found in the equivalent diastereomers, (2*R*, 3*R*) and/or (2*S*, 3*S*). Single-crystal X-ray diffraction data were collected at low temperature with Cu Kα radiation ($\lambda = 1.54184$ Å). Optically active: monoclinic, space group *C*2, with $a = 24.726(3)$, $b = 5.2426(5)$, $c = 12.0726(12)$ Å, $\beta = 112.979(9)°$, $V = 1440.8(5)$ Å^3, $Z = 4$, $D_x = 1.389$ g cm^{-3}, $\mu = 20.35$ cm^{-1}, the refinement on 2918 observed reflections gave $R = 0.0271$. Racemic: monoclinic, space group $P2_1/n$, with $a = 13.308(3)$, $b = 4.8474(8)$, $c = 22.130(4)$ Å, $\beta = 91.782(14)$, $V = 1426.9(5)$ Å^3, $Z = 4$, $D_x = 1.403$ g cm^{-3}, $\mu = 20.54$ cm^{-1}, refined to $R = 0.0318$ for 2753 observed reflections. An intramolecular hydrogen bond between the hydroxy and carbonyl groups appears to stabilize the benzothiazepinone ring in the (*P*,2*S*,3*R*) boat conformation with the hydroxy and methoxyphenyl substituents in equatorial positions. In both crystal structures two N–H···O hydrogen bonds connect the molecules into dimers. In the optically active compound the two molecules are related by a twofold axis, in the racemate by an inversion centre. The racemate contains an additional hydrogen bond which is reflected by its higher melting enthalpy compared with the optically active compound. The difference in the chiral discrimination in the solutions of the *cis*-and *trans*-diastereomers does not appear to have its origin in the strong (O–H···O, N–H···O) hydrogen bonds, but rather in the weak (C–H···O) interactions.

Molecules with one chiral centre can exist as two stereoisomers classified by the absolute configuration *S* and *R*. The two forms are enantiomers, i.e., non-superimposable mirror images of each other. Introducing an additional different chiral centre gives rise to four (*SS*, *SR*, *RS* and *RR*) stereoisomers, related as enantiomers and diastereomers. If the two chiral centres are adjacent and part of a cyclic system the stereoisomers are frequently classified as *cis* and *trans* diastereomers. In this case the constraints of the ring system may cause a difference in the overall conformations of the diastereomers due to the intra- and inter-molecular interactions.

In the simplest case one would expect that the crystallization of four such stereoisomers would lead to four different crystal structures: enantiomeric (*RR* or *SS*), racemic (*RR* and *SS*), enantiomeric (*RS* or *SR*) and racemic (*RS* and *SR*). Knowledge of the four different crystal structures of such a system enables comparisons to be made between enantiomers and racemates and between the different diastereomers. This type of analysis may in turn be related to the chiral discrimination observed with other techniques.

For 3-hydroxy-2-(4-methoxyphenyl)-2,3-dihydro-1,5-benzothiazepin-4(5*H*)-one (**1**) it was possible to isolate all four crystal forms of enantiomers and racemates.

[†] Deceased.

[‡] The Centre for Crystallographic Studies is funded by The Danish National Research Foundation.

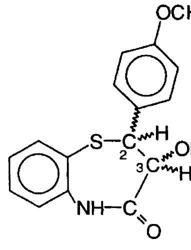

1

cis
(2*S*, 3*S*)
(2*SR*, 3*SR*)

trans
(2*S*, 3*R*)
(2*SR*, 3*RS*)

It has previously been shown that the enantiomeric purity of *cis*-**1** could be determined without the use of an auxiliary chiral reagent from the ^{1}H NMR spectra in concentrated solutions made up with aprotic solvents, indicating associations between molecules. We have investigated the crystal structures of racemic and optically active *cis*-**1** in order to elucidate this aspect.[1]

The change of absolute configuration on one of the carbon atoms causes significant changes in the properties of **1**. The ^{1}H NMR spectra of the *trans* diastereomer, measured under a wide range of conditions, did not indicate any associations between the enantiomers.[2] Therefore we found it important to undertake a similar investigation of the solid state structures of the *trans* isomers of **1**, which do not show evidence of molecular associations in solution, to place our previous results for the *cis*-isomers into proper perspective.

We report here the crystal structures of (2*S*,3*R*)-and (2*SR*,3*RS*)-**1** and use the knowledge of the structures of the four stereoisomers to compare their stereochemistry. These results are related to the ability of the molecules to associate in aprotic solvents.

Experimental

Preparation. 2.0 g (6 mmol) (2*SR*,3*RS*)-3-(2-aminophenylthio)-2-hydroxy-3-(4-methoxyphenyl)propionic acid[3] were dissolved in xylene and refluxed for 11 h. Water was removed by use of a 'Dean–Stark' trap. After cooling, the crystals were removed by filtration, washed with cold ethanol and dried. Yield: 0.79 g (42%). After recrystallization from ethanol the m.p. was 204–205 °C.

(2*S*,3*R*)-**1** was prepared similarly to the racemate starting from 2 g (6 mmol) (2*S*,3*R*)-3-(2-aminophenylthio)-2-hydroxy-3-(4-methoxyphenyl)propionic acid.[3] Yield: 1.24 g (66%). The $[\alpha]_D^{20} = -837.0$ ($c = 0.5$, DMF), and the m.p. was 193–194 °C after recrystallization from methanol.

Crystals for the single crystal diffraction study were grown from abs. ethanol containing 5% acetone.

Spectroscopic measurements. Optical rotations were measured at room temperature at 589 nm (Na$_D$) with a Perkin Elmer 241 polarimeter.

Thermodynamic measurements. Melting points and heats of fusion were measured by differential scanning calorimetry using a PL-DSC instrument calibrated with indium and tin. The measurements were carried out under a nitrogen atmosphere in open crucibles. Sampling was done every 1.25 s and a heating rate of 5 K min^{-1} was used. The mass of each sample was between 3.8 and 3.9 mg measured with a precision of 0.001 mg. The error of the melting point determination is ± 0.5 K. The heat of fusion could be determined to a reproducibility of 5%. Thermogravimetric measurements on the samples showed no decomposition in the temperature range investigated.

X-ray powder diffraction patterns. A STOE Stadi P powder diffractometer was used to record the diagrams of (2*S*,3*R*)-and (2*SR*,3*RS*)-**1** using Cu Kα_1 radiation selected by a curved germanium monochromator. The diffraction patterns from the samples recorded in a transmission mode were measured with a position-sensitive detector covering 7° in 2θ . The software[4] Visual X$^{\mathrm{POW}}$ supplied with the instrument was used to analyse the diffraction patterns, which were found to be in agreement with the results obtained from the single crystal X-ray diffraction study.

Structure determinations. The data collections for both compounds were performed with a CAD4 diffractometer. Cu Kα ($\lambda = 1.54184$ Å) radiation obtained from a graphite monochromator was used. The crystals were cooled with an Enraf–Nonius gas-flow low-temperature device. The temperature, monitored with a thermocouple placed a few centimetres above the crystal in the exhaust pipe, was 110 K for the (−)-(2*S*,3*R*)-**1** crystal and 122 K for the (2*SR*,3*RS*)-**1** crystal, in both cases the variations were to within 1 K. The different experimental conditions with a summary of the results from data reduction and structure refinement are presented in Table 1. An analysis of reflection profiles provided the basis for the selection of ω–2θ scan mode and scan interval for both data collections, which also included measurements of three standard reflections every 10 000 s. The orientation of the crystals was checked after every 300 reflections. Different crystallographic program packages were used for each structure.

*(−)-(2S,3*R*)-**1**.* The data reduction included corrections for background, Lorentz and polarization effects. The intensities of the standard reflections did not show any systematic variations. Unfortunately the crystal was lost after data collection so only its approximate dimensions were known, therefore the data reduction did not include corrections for absorption effects. Reflections related by the symmetry of the crystal class were averaged. The crystal structure was solved by direct methods[5] and refined by full-matrix least-squares minimizing $\Sigma w(|F_o|\text{-}|F_c|)^2$. After anisotropic displacement parameters had been introduced, the difference electron density showed the positions of all the hydrogen atoms in the

Table 1. Crystal data and summary of the data collection and structure refinement results.

	(−)-(2*S*,3*R*)	(±)-(2*SR*,3*RS*)
Formula	$C_{16}H_{15}NO_3S$	$C_{16}H_{15}NO_3S$
Formula weight	301.35	301.35
T/K	110±1	122±1
Space group	*C*2	*P*2$_1$/*n*
a/Å	24.726(3)	13.308(3)
b/Å	5.2426(5)	4.8474(8)
c/Å	12.0726(12)	22.130(4)
β/°	112.979(9)	91.782(14)
V/Å^3	1440.8(5)	1426.9(5)
Z	4	4
F(000)	632	632
Crystal size/mm	0.05×0.13×0.25	0.07×0.24×0.48
D_x/g cm^{-3}	1.389	1.403
μ(Cu Kα)/mm^{-1}	2.035	2.054
Refl. used in determ. of cell parameters	22	22
θ range/°	35.99-46.05	38.82-43.08
Scan type	ω−2θ	ω−2θ
Standard reflections	(4,0,0) (1,1,0) (0,0,2)	(2,0,0) (0,1,2) (0,0,8)
θ range for data collection/°	1-75	1-75
Range of *h*	−30-30	0-16
Range of *k*	−6-6	−6-6
Range of *l*	−15-15	−27-27
R_{int}	0.024	0.026
Number of measured reflections incl. standard reflections	5343	5374
Number of independent reflections	3028	2826
Number of observed reflections [$I>2\sigma(I)$]	2918	2753
Number of variables	234	236
R for $F>4\sigma(F)$	0.027	0.032
max. shift/e.s.d.	0.04	0.002
max. and min. Δρ/e Å^{-3}	0.50 and −0.45	0.44 and −0.32

structure. Their positional parameters were included in the refinement with a fixed isotropic displacement parameter of 2.5 Å^2. The absolute configuration was chosen to match the absolute configuration known from the synthesis of (−)-(2*S*,3*R*)-3-acetoxy-5-(2-dimethylaminoethyl)-2-(4-methoxyphenyl)-2,3-dihydro-1,5-benzothiazepin-4(5*H*)-one hydrochloride[6] and it was in agreement with the absolute configuration determined as described by Rogers.[7] A weighting scheme of $[\sigma_s^2(F)+0.0006F^2]^{-1}$ was used and the final refinement cycle resulted in an R_w and *S* for all $F^2>2\sigma(F^2)$ of 0.036 and 1.164, respectively. Apart from the structure determination all crystallographic computations were performed with the SDP-system.[8]

*(±)-(2*SR*,3*RS*)-1.* The data reduction performed with the DREADD programs,[9] included corrections for degradation, Lorentz, polarization, background and absorption effects. The transmission factors were in the range 0.491–0.870. Reflections related by the symmetry of the crystal class were averaged. The structure was solved by direct methods using SHELXS-86[5] and refined by full matrix least-squares with SHELXL-93[10] minimizing $\Sigma w(F_o^2-F_c^2)^2$. Scattering factors were taken from Ref. 11 and used as contained in the program. After anisotropic displacement parameters had been introduced for the non-hydrogen atoms, the difference Fourier map showed the positions of all the hydrogen atoms. The positional parameters of the hydrogen atoms were included in the refinement using an isotropic displacement parameter made equal to U_{eq} of the parent atom multiplied by 1.5 for the hydroxy and methoxy hydrogen atoms and 1.2 for the remaining hydrogen atoms. The final cycles of the refinement included an isotropic extinction coefficient which resulted in a final value of 0.0072(5) Å^{-3}. The suggested weighting scheme of $[\sigma^2(F_o^2)+(0.0543P)^2+0.6179P]^{-1}$ where $P=[\max.(F_o^2,0)+2F_c^2]/3$ was used and the final refinement cycle resulted in a wR_2 and *S* for all F^2 data of 0.0888 and 1.064, respectively. The difference electron density map calculated after the final cycles of refinement had the highest peaks between bonded atoms and the lowest troughs adjacent to S.

The final atomic coordinates are listed in Table 2. Anisotropic displacement parameters, parameters for the

Table 2. Atomic coordinates and equivalent isotropic displacement parameters (Å^2) for optically active and racemic *trans*-**1**.

	x	y	z	U_{eq}[a]
(−)-(2*S*,3*R*)-**1**				
S1	0.62147(1)	0.500	0.84592(2)	0.01608(6)
O1	0.47169(4)	0.8219(2)	0.62073(8)	0.0226(3)
O2	0.49973(4)	1.0266(2)	0.84206(8)	0.0180(3)
O4	0.67288(5)	0.7869(2)	1.39777(8)	0.0223(3)
N1	0.56498(5)	0.8622(3)	0.63309(9)	0.0181(3)
C1	0.52437(5)	0.8574(3)	0.6819(1)	0.0167(3)
C2	0.54491(5)	0.9095(3)	0.8166(1)	0.0144(3)
C3	0.56699(5)	0.6644(3)	0.8910(1)	0.0128(3)
C4	0.66972(7)	0.5835(3)	1.4737(1)	0.0276(4)
C11	0.59132(5)	0.7068(3)	1.0251(1)	0.0134(3)
C12	0.62847(5)	0.9130(3)	1.0796(1)	0.0149(3)
C13	0.65373(6)	0.9353(3)	1.2042(1)	0.0163(3)
C14	0.64326(6)	0.7527(3)	1.2765(1)	0.0163(3)
C15	0.60542(6)	0.5498(3)	1.2243(1)	0.0172(3)
C16	0.57988(5)	0.5293(3)	1.0991(1)	0.0144(3)
C21	0.65656(5)	0.7500(3)	0.8018(1)	0.0141(3)
C22	0.62629(5)	0.8946(3)	0.6982(1)	0.0153(3)
C23	0.65608(6)	1.0668(3)	0.6555(1)	0.0184(3)
C24	0.71628(6)	1.0984(3)	0.7151(1)	0.0201(3)
C25	0.74679(5)	0.9613(3)	0.8195(1)	0.0194(3)
C26	0.71731(6)	0.7880(3)	0.8631(1)	0.0168(3)
(±)-(2*SR*,3*RS*)-**1**				
S1	1.09235(2)	0.97179(7)	0.314428(13)	0.01797(13)
O1	0.90284(7)	0.9301(2)	0.44613(4)	0.0235(2)
O2	0.84038(7)	0.5673(2)	0.36142(4)	0.0234(2)
O4	0.85685(7)	0.2812(2)	0.08872(4)	0.0265(2)
N1	1.06274(8)	0.7695(3)	0.44450(5)	0.0198(2)
C1	0.96910(9)	0.7970(3)	0.42113(5)	0.0182(3)
C2	0.94216(9)	0.6473(3)	0.36209(5)	0.0171(3)
C3	0.96329(9)	0.8358(3)	0.30758(5)	0.0167(3)
C4	0.92510(12)	0.0907(4)	0.06292(7)	0.0300(3)
C11	0.93927(9)	0.6931(3)	0.24816(5)	0.0169(3)
C12	1.00397(10)	0.4980(3)	0.22460(6)	0.0180(3)
C13	0.98002(10)	0.3563(3)	0.17138(6)	0.0192(3)
C14	0.88926(10)	0.4109(3)	0.14109(5)	0.0190(3)
C15	0.82405(10)	0.6089(3)	0.16342(6)	0.0212(3)
C16	0.84908(10)	0.7484(3)	0.21642(6)	0.0195(3)
C21	1.16110(9)	0.7102(3)	0.35356(5)	0.0165(3)
C22	1.14299(9)	0.6435(3)	0.41385(6)	0.0185(3)
C23	1.20386(10)	0.4526(3)	0.44462(6)	0.0233(3)
C24	1.28291(10)	0.3290(3)	0.41537(7)	0.0261(3)
C25	1.30187(10)	0.3944(3)	0.35567(6)	0.0241(3)
C26	1.24125(9)	0.5838(3)	0.32506(6)	0.0204(3)

[a] U_{eq} is defined as one third of the trace of the orthogonalized U_{ij} tensor.

hydrogen atoms and lists of the observed and calculated structure factors can be obtained from the authors (S.L.).

Results and discussion

A description of the molecular conformations found in (2*SR*,3*RS*)-**1** and (2*S*,3*R*)-**1** is presented first with a comparison of the intermolecular interactions and packing in the two crystal structures. The observed differences in the hydrogen bonding patterns are then related to the differences in the thermochemical properties. Finally the structural results are compared with previously reported crystal structures of racemic and optically pure *cis*-**1**.

Molecular geometry. The molecular geometries of *trans*-**1** found in the crystal structures of (2*SR*,3*RS*)-**1** and (2*S*,3*R*)-**1** are illustrated by the bond lengths, angles and torsion angles in Table 3 and the drawings in Figs. 1 and 2. The difference between the two C–S distances of the seven-membered ring reflects the sp^2 and sp^3 character of the two carbon atoms. The slightly longer O1–C1 distance and the slightly shorter C1–N1 distance, compared with the normal values for a C=O double and C–N single bond reveal pronounced conjugation within the C22–N–C1–O1 fragment. The bond lengths and angles are virtually identical for *trans*-**1** in its racemic and optically active crystal forms, the only significant

Table 3. Bond distances (Å), bond angles and selected torsion angles (°) in **1**.

	(−)-(2*S*,3*R*)	(±)-(2*SR*,3*RS*)
S1-C21	1.7654(14)	1.7737(13)
S1-C3	1.8511(13)	1.8416(13)
O1-C1	1.235(2)	1.237(2)
O2-C2	1.410(2)	1.409(2)
O4-C14	1.369(2)	1.376(2)
O4-C4	1.428(2)	1.427(2)
N1-C1	1.348(2)	1.341(2)
N1-C22	1.419(2)	1.421(2)
C1-C2	1.527(2)	1.527(2)
C2-C3	1.541(2)	1.546(2)
C3-C11	1.507(2)	1.511(2)
C11-C12	1.405(2)	1.391(2)
C11-C16	1.393(2)	1.398(2)
C12-C13	1.390(2)	1.392(2)
C13-C14	1.387(2)	1.388(2)
C14-C15	1.394(2)	1.395(2)
C15-C16	1.397(2)	1.386(2)
C21-C26	1.406(2)	1.397(2)
C21-C22	1.403(2)	1.401(2)
C22-C23	1.385(2)	1.393(2)
C23-C24	1.387(2)	1.388(2)
C24-C25	1.391(2)	1.390(2)
C25-C26	1.391(2)	1.385(2)
C21-S1-C3	104.07(6)	104.46(6)
C14-O4-C4	116.60(12)	116.48(11)
C1-N1-C22	125.23(11)	124.19(11)
O1-C1-N1	122.21(12)	123.10(12)
O1-C1-C2	119.88(12)	118.60(11)
N1-C1-C2	117.85(11)	118.25(11)
O2-C2-C1	110.33(11)	109.88(10)
O2-C2-C3	111.51(10)	110.65(10)
C1-C2-C3	111.52(11)	110.08(10)
C11-C3-C2	113.91(11)	111.72(10)
C11-C3-S1	110.69(9)	114.02(8)
C2-C3-S1	110.47(9)	109.82(8)
C12-C11-C16	118.21(12)	118.29(12)
C12-C11-C3	122.05(12)	121.37(11)
C16-C11-C3	119.63(12)	120.31(11)
C11-C12-C13	120.47(13)	121.63(12)
C14-C13-C12	120.51(13)	119.18(12)
O4-C14-C13	115.42(13)	124.39(12)
O4-C14-C15	124.61(13)	115.50(11)
C13-C14-C15	119.97(12)	120.11(12)
C16-C15-C14	119.21(12)	119.99(12)
C15-C16-C11	121.57(13)	120.79(12)
C26-C21-C22	118.82(12)	119.01(12)
C26-C21-S1	119.73(11)	118.85(10)
C22-C21-S1	121.08(10)	121.91(10)
C23-C22-C21	120.49(12)	120.27(12)
C23-C22-N1	118.70(12)	119.10(12)
C21-C22-N1	120.79(12)	120.63(12)
C24-C23-C22	120.28(13)	119.75(13)
C23-C24-C25	120.03(13)	120.49(14)
C26-C25-C24	120.14(13)	119.75(13)
C25-C26-C21	120.21(13)	120.73(12)
S1-C3-C2-C1	51.13(13)	51.46(12)
C3-C2-C1-N1	−86.1(2)	−90.55(14)
C2-C1-N1-C22	4.6(2)	9.5(2)
C1-N1-C22-C21	48.4(2)	46.3(2)
N1-C22-C21-S1	6.8(2)	5.0(2)
C22-C21-S1-C3	−67.99(12)	−66.80(11)
C21-S1-C3-C2	31.31(10)	30.55(10)
S1-C3-C2-O2	174.97(8)	173.11(9)
C1-C2-C3-C11	176.44(11)	179.00(10)
O1-C1-C2-O2	−28.0(2)	−630.3(2)
O1-C1-C2-C3	96.5(2)	91.81(14)
O1-C1-N1-C22	−178.07(14)	−172.93(13)
S1-C3-C11-C12	82.10(14)	47.8(2)
S1-C3-C11-C16	−93.97(14)	−134.37(11)
C2-C3-C11-C12	−43.1(2)	−77.5(2)
C2-C3-C11-C16	140.84(13)	100.38(14)
C13-C14-O4-C4	−171.19(14)	−3.8(2)
C15-C14-O4-C4	7.8(2)	176.11(13)

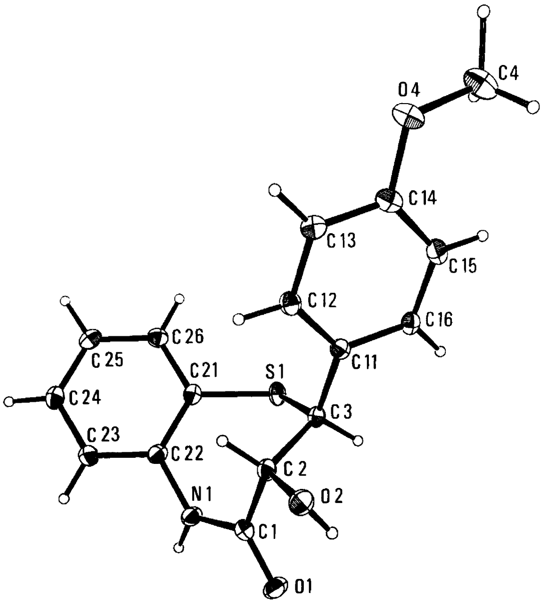

Fig. 1. ORTEPII[12] drawing showing the molecular geometry of (−)-(2*S*,3*R*)-**1**. The thermal ellipsoids are scaled to include 50% probability. The hydrogen atoms are drawn as spheres of fixed radius.

differences are related to the different orientation of the methoxy group relative to the phenyl ring. *trans*-**1** adopts a different conformation in the crystals of the racemate and the pure enantiomer as reflected by the relative orientation of the *p*-methoxyphenyl group, the torsion angle S1–C3–C11–C12 is 82.10(14) and 47.8(2) in (2*S*,3*R*)-**1** and (2*SR*,3*RS*)-**1**, respectively.

Among the possible conformers for the seven-membered ring it is found that it takes a (*P*,2*S*,3*R*) boat conformation in (2*SR*,3*RS*) and (2*S*,3*R*)-**1**. This is in contrast with the *cis* diastereomers where the benzothiazepinone rings adopt a twist–boat conformation in the optically active form and the racemate.[1] A salt of a derivative of **1**, 3-acetoxy-5-(2-dimethylaminoethyl)-2-(4-methoxyphenyl)-2,3-dihydro-1,5-benzothiazepin-4(5*H*)-one hydrochloride has been reported to adopt a twist–boat conformation in its optically active *cis*[13] and *trans*[6] diastereomers, this conformation being predicted to have the lowest energy from molecular-mechanics calculations.[14]

An intramolecular O2–H2O···O1 interaction (see Table 4) is observed in racemic and optically active crystals of *trans*-**1**. This appears to stabilize the (*P*,2*S*,3*R*) conformer which has the hydroxy and *p*-methoxyphenyl groups in equatorial positions. It is noteworthy that this particular type of intramolecular interaction suggested for *cis*-(2*S*,3*S*)-3-hydroxy-5-(2-dimethylaminoethyl)-2-(4-methoxyphenyl)-2,3-dihydro-1,5-benzothiazepin-4(5*H*)-one derivatives[15] was not observed in the crystal structures of racemic and optically active *cis*-**1**.[1]

*Crystal packing in the crystal structures of (2*SR,3*RS) and (2*S,3*R)-*1. The strongest intermolecular interactions in both racemic and optically active *trans*-**1** are two N1–H1N···O1 hydrogen bonds that connect two molecules into dimers (see Table 4 and Figs. 3 and 4.) In the optically active form the molecules in the dimers are related by a crystallographic twofold axis whereas an inversion centre relates them in the racemate. An additional O2–H2O···O4 hydrogen bond links the molecules related by a twofold screw axis in the racemate. Although the hydrogen bond geometry of the dimers is very similar it leads to different packing in the two structures.

Table 4. Hydrogen bond dimensions in *trans*-**1**.

D–H···A	D···A/Å	D–H···A/Å	H···A/Å
(−)-(2*S*,3*R*)-**1**			
N1–H1N···O1[a]	2.844(2)	178(2)	1.97(2)
O2–H2O···O1	2.7066(14)	106(2)	2.39(2)
(±)-(2*SR*,3*RS*)-**1**			
N1–H1N···O1[b]	2.849(2)	174(2)	2.02(2)
O2–H2O···O1	2.684(1)	117(2)	2.21(2)
O2–H2O···O4[c]	3.060(2)	139(2)	2.38(2)

[a] 1−*x*, *y*, 1−*z*. [b] 2−*x*, 2−*y*, 1−*z*. [c] 1.5−*x*, *y*+0.5, 0.5−*z*.

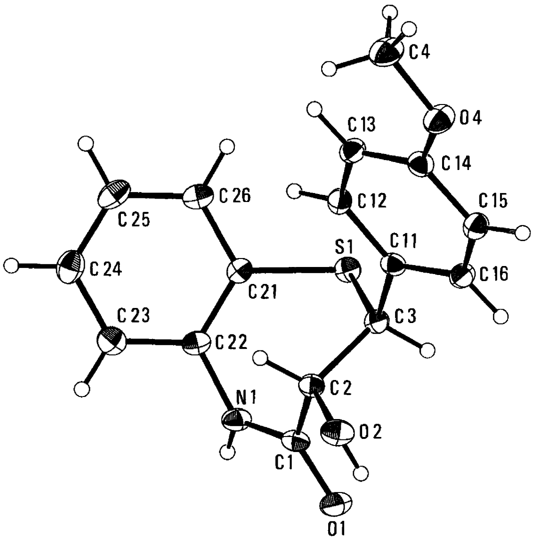

Fig. 2. ORTEPII[ort] drawing showing the molecular geometry of (±)-(2*SR*,3*RS*)-**1**. The thermal ellipsoids are scaled to include 50% probability. The hydrogen atoms are drawn as spheres of fixed radius.

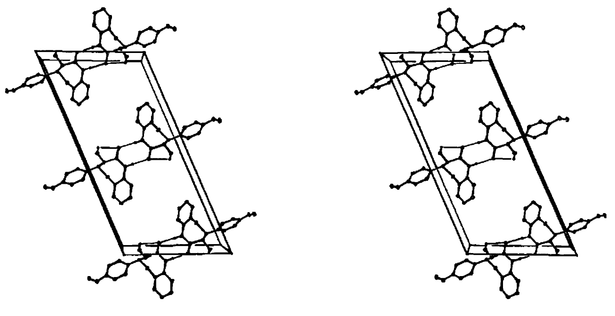

Fig. 3. Stereopair[12] illustrating the packing in (−)-(2*S*,3*R*)-**1** viewed along the *b* axis. The hydrogen bonds are shown as thin lines. Hydrogen atoms not involved in the hydrogen-bonding scheme are omitted for clarity.

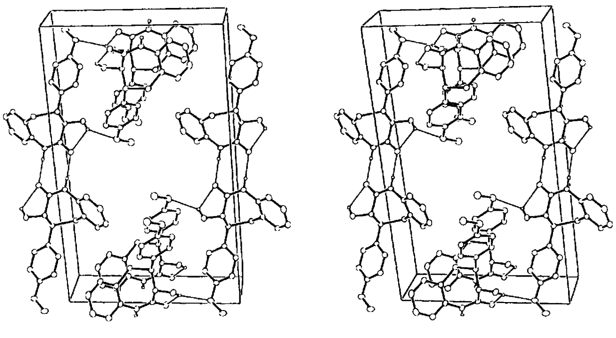

Fig. 4. Stereopair[12] illustrating the packing in (±)-(2*SR*,3*RS*)-**1** viewed along the *b* axis. The hydrogen bonds are shown as thin lines. Hydrogen atoms not involved in the hydrogen-bonding scheme are omitted for clarity.

Thermochemical properties. The melting points and melting enthalpies measured by DSC were used to calculate the melting entropies of (2*SR*,3*RS*)-**1** and (2*S*,3*R*)-**1** and construct the binary phase diagram by the Schröder–Van Laar and Prigogine–Defay equations[16] shown in Fig. 5. The eutectic was calculated to have a composition $x_{\mathrm{eu}} = 0.14$, and a melting point $T_{\mathrm{eu}} = 460.3$ K.

The shape of the binary phase diagram reflects the 4.2 kJ mol^{-1} difference in the melting enthalpies of (2*SR*,3*RS*)- and (2*S*,3*R*)-**1**. One might expect that the additional O2–H2O···O4 hydrogen bond observed in (2*SR*,3*RS*)-**1** would account for an energy difference of this magnitude.

Comparison of the enantiomer associations in racemic and optically active cis- *and* trans-**1**. The optical purity of *cis*-**1** could be determined by ^{1}H NMR spectroscopy in apolar solvents without the use of chiral agents, using the signals of the *p*-methoxy protons. In enantiomeric mixtures where the composition differs from 1 : 1, two sets of signals were observed for the *p*-methoxy and aromatic protons. This is explained as being due to the formation of homochiral (*SS*,*SS* or *RR*,*RR*) and heterochiral (*SS*,*RR*) dimers by two identical N–H···O hydro-

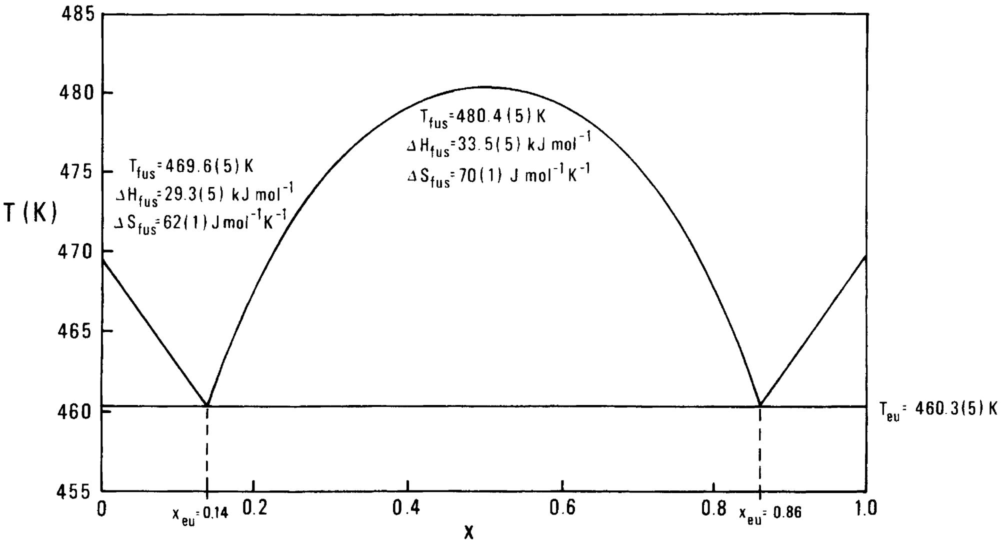

Fig. 5. Binary phase diagram calculated with the Schröder–Van Laar and Prigogine–Defay equations[16] based on the melting point and melting enthalpies measured by DSC.

gen bonds.[2] Since it is plausible that the strongest intermolecular interactions in an aprotic solvent are preserved in the solid state, we investigated the crystal structures of *cis*-**1**.[1] The subsequent analysis revealed that the predicted dimers do not exist in these crystal structures but instead intermolecular O–H···O and N–H···O hydrogen bonds connect molecules of identical chirality into infinite chains. A C–H···O hydrogen bond between one of the methoxy hydrogen atoms and the hydroxy oxygen in optically active *cis*-**1** seems to be the origin of the non-equivalence of the ^{1}H NMR spectra.

Giordano *et al.*[2] did not observe self-discrimination of the enantiomers in the *trans*-diastereomer. The structure determinations reported here reveal that the crystal structure of racemic *trans*-**1** contains heterochiral dimers, whereas optically active *trans*-**1** contains dimers of molecules of the same handedness. It is noteworthy that dimers of this type were earlier suggested to be the origin of the difference in the ^{1}H NMR spectra of the *cis*-isomer.

Knowledge of the crystal packing in the structures of the four stereoisomers of **1** demonstrates that one should be careful in using a simple picture of enantiomer associations to interpret solution properties. Furthermore, we note that the formation of homo- and hetero-chiral motifs in the crystal structures of enantiomers and racemates does not necessarily imply the possibility of optical purity determination in solution.

The crystal structure determinations of racemic and optically active *trans*-**1** substantiate the assertion that the formation of strongly hydrogen-bonded homo and hetero dimers in the solid state does not necessarily make it possible to detect these associations in solution. Our results on the *cis* diastereomer indicate that chiral discrimination may instead be caused by weak C-H···O interactions.

Acknowledgements. This research was supported by the Danish Natural Science Research Council by a grant to S.L. and by the OTKA grant T-4183 to M.Á. and E.F. We thank the Faculty of Science, University of Copenhagen for financial support to K.M. The assistance of Flemming Hansen in the experimental crystallographic work is gratefully acknowledged. The thermoanalytical equipment was made available through a grant from the Lundbeck Foundation and the powder diffractometer by a grant from the Danish Natural Science Research Council.

References

1. Marthi, K., Larsen, S., Ács, M. and Fogassy, E. *J. Mol. Struct. 374* (1996) 347.
2. Giordano, C., Restelli, A., Villa, M. and Annunzita, R. *J. Org. Chem. 56* (1991) 2270.
3. Jászay, Zs. *Unpublished results.*
4. Visual X^{POW} software package for STOE Powder Diffraction System STADI P, STOE & CIE GmbH, Darmstadt, Germany 1994.
5. Sheldrick, G. M. *Acta Crystallogr., Sect. A 46* (1990) 467.
6. Tanaka, T., Inoue, H., Date, T., Okamura, K., Aoe, K., Takeda, M., Kugita, H., Murata, S., Yamaguchi, T., Kikkawa, K., Nakajima, S. and Nagao, T. *Chem. Pharm. Bull.* 40 (1992) 1476.
7. Rogers, D. *Acta Crystallogr., Sect. A 37* (1981) 734.
8. *Enraf-Nonius SDP-Plus Structure Determination Package,* Enraf-Nonius, Delft, The Netherlands 1985.
9. Blessing, R. H. *Cryst. Rev. 1* (1987) 3.
10. Sheldrick, G. M. *J. Appl. Cryst.* (1995). *In preparation.*
11. *International Tables for X-ray Crystallography,* Kluwer, Dordrecht 1992, Vol. C.
12. Johnson, C. K. *ORTEPII Report ORNL-5138,* Oak Ridge National Laboratory, Tennessee, USA 1976.
13. Koji-Prodi, B., Ružić-Toroš, Ž., Šunjić, V., Decorte, E. and Moimas, F. *Helv. Chim. Acta 67* (1984) 916.

14. Glaser, R. and Sklarz, B. *J. Chem., Soc., Perkin Trans. 2.* (1989) 1031.
15. Bozolli, A., Marotta, E., Piani, S. and Rosini, G. *Tetrahedron Lett. 34* (1993) 3759.
16. Jacques, J., Collet, A. and Wilen, S. H. *Enantiomers, Racemates, and Resolutions,* Wiley, New York 1981, pp. 46, 91.

Received January 29, 1996.